Macroscopic Manipulation of High-Order-Harmonic Generation Through Bound-State Coherent Control

Itai Hadas and Alon Bahabad*

Department of Physical Electronics, School of Electrical Engineering, Iby and Aladar Fleischman Faculty of Engineering, Tel-Aviv University, Tel-Aviv 69978, Israel

(Received 28 May 2014; published 19 December 2014)

We propose a paradigm for macroscopic control of high-order harmonic generation by modulating the bound-state population of the medium atoms. A unique result of this scheme is that apart from regular spatial quasi-phase-matching (QPM), also purely temporal QPM of the emitted radiation can be established. Our simulations demonstrate temporal QPM by inducing homogenous Rabi oscillations in the medium and also spatial QPM by creating a grating of population inversion using the process of rapid adiabatic passage. In the simulations a scaled version of high-order harmonic generation is used: a far off-resonance 2.6 μm source generates UV-visible high-order harmonics from alkali-metal-atom vapor, while a resonant near IR source is used to coherently control the medium.

DOI: 10.1103/PhysRevLett.113.253902 PACS numbers: 42.65.Ky, 32.80.Xx, 37.10.Jk

High-order harmonic generation (HHG) is an extreme nonlinear process in which a medium ionized by a short ionizing laser pulse emits attosecond pulses made of up-converted harmonics of the pump frequency [1,2]. HHG has become a valuable research resource due to its ability to pump and probe electronic dynamics in single atoms and molecules [2,3].

In many cases frequency-conversion processes suffer from low conversion efficiency due to dispersion induced phase mismatch between the pump and the converted emission. Quasi-phase-matching (QPM) [4] is a macroscopic manipulation technique which applies a systematic correction to the phase mismatch, increasing significantly the conversion efficiencies. In the last two decades various QPM schemes have been experimentally demonstrated for HHG. In all of these cases a periodic modulation of either the medium [5–8] or pump field [9–11] was used. Traditionally, the phase mismatch of the nonlinear process is interpreted as a momentum imbalance between the interacting photons while QPM provides a spatial modulation to replace momentum conservation with the less restricting quasimomentum conservation [12]. In 2010, it was shown [13] that the phase mismatch can also be cast in the form of an energy imbalance, requiring QPM to provide a temporal modulation. That work showed that a previous experiment [10] demonstrating all-optical QPM using a train of counterpropagating pulses was actually employing a spatiotemporal modulation to fix both a momentum and an energy mismatch. To date, purely temporal QPM is yet to be demonstrated.

Here we propose to use coherent control [14,15] on the bound-state electronic population of the medium's atoms (or molecules) to establish macroscopic control of HHG. Thus QPM would be achieved through modulation of the internal state of the medium's atoms. Depending on the type of modulation, either spatial or purely temporal QPM would be established.

We mention that extensive work has been done on HHG from an excited medium. Some interesting phenomena have been simulated and observed such as the increase of the harmonic yield in comparison with a medium initially in its ground state [16–20], increase of the cutoff energy [20,21], generation of single attosecond pulses [20,22], generation of two distinctive harmonic plateaus with different conversion efficiencies [23,24], and for controlling and monitoring attosecond scale electron dynamics [25,26]. There have also been studies of the contribution of different channels within a superposition state to the HHG spectrum [27,28]. Here a HHG channel is defined by the bound state from which an electron is being ionized and the bound state to which it recombines to emit the harmonic radiation. For an initially unexcited medium the only channel is the ground-ground (gg) channel, while for an excited medium with a single excited state (e) there are three more possible channels: ge, eg, and ee (see Fig. 1). Macroscopically, spatial population gratings have been used for HHG transient grating spectroscopy, allowing us to extract the amplitude and phase dynamics of excited rotational or vibrational molecular states at low excitation levels [29–32]. Finally, it was suggested to use a transient molecular alignment grating as a spatial QPM for the process of third harmonic generation [33].

Here we show how a coherent manipulation of the electronic population of two bound states together with the process of HHG, can achieve macroscopic control in the form of spatial or temporal QPM of the emitted high-order harmonics radiation. Let us first consider an excited medium, with constant ground and excited state populations, $|a_g|^2$ and $|a_e|^2$, respectively, where a_g and a_e are the appropriate probability (population) amplitudes. Expending

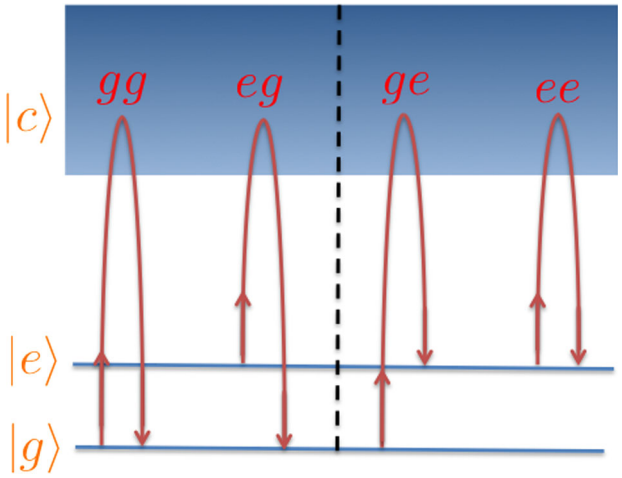

FIG. 1 (color online). Four channels of HHG from a two-level system. g is the ground state of the atom, e is the first excited state, and c represents continuum states. Each channel includes the ionization of an electron from one of the bound states to the continuum and its recombination into a bound state, e.g., ge means that an electron is ionized from the ground state of the atom and recombines into the excited state. The dashed line separates channels which have different phase mismatch values in case the index of refraction changes during the interaction.

a previously used single atom nomenclature [28] to the macroscopic domain, we write the polarization of the medium for a specific qth harmonic order as

$$P(z,t;\omega_q) \propto e^{i\Delta\phi_g(z,t)}[|a_g|^2 d_{gg}(\omega_{q,g}) + a_g^* a_e d_{eg}(\omega_{q,g})] + e^{i\Delta\phi_e(z,t)}[|a_e|^2 d_{ee}(\omega_{q,e}) + a_g a_e^* d_{ge}(\omega_{q,e})], \quad (1)$$

where $d_{ij}(\omega_q)$ is the Fourier component of the dipole moment matrix element for the ij channel ($i,j \in \{e,g\}$) at frequency $\omega_{q,i} = q\omega_0 - \Delta\omega_i$, ($i \in \{e,g\}$). ω_0 is the HHG pump frequency, and $\Delta\omega_i$ is the energy mismatch [13]. $\Delta\phi_g$ and $\Delta\phi_e$ are the phase mismatch values associated with channels which recombine to the g state and to the e state, respectively. An electron recombining to state g or to state e would lead to the emission of different photon energies. Thus the emission of the same photon energy while recombining to different bound states could only be the result of different electron trajectories—hence the time of recombination would be different for the two cases. Because in general the dispersion in a medium experiencing ionization is time dependent, the associated phase mismatch values would be time dependent as well. The general expression for a spatiotemporal phase mismatch is [13] $\Delta\phi_i = \Delta k_i z - \Delta\omega_i t$, where Δk_i and $\Delta\omega_i$ are the momentum and energy mismatch components, respectively. For traditional spatial QPM, $\Delta\omega$ is zero, while for purely temporal QPM, Δk is zero. The dispersion relation for the phase mismatch components is [13]

$$\Delta k_i = \frac{n(\omega_{q,i})}{c}\Delta\omega_i + \frac{q\omega_0}{c}[n(\omega_0) - n(\omega_{q,i})] \quad (2)$$

where $n(\omega)$ is the index of refraction. The phase mismatch terms preclude the polarization terms in different interaction coordinates to be added in phase. To establish QPM we modulate the population amplitudes. This modulation can be spatial, temporal or spatiotemporal for the appropriate desired type of QPM. It is important to understand that this modulation is done quasistatically with regards to the interaction of the atoms with the HHG pump. From the perspective of any single atom in the medium, the coherent control beam prepares the population distribution between the bound states towards the interaction with the HHG pump beam.

To establish purely temporal QPM, we suggest to irradiate the medium uniformly with a close to resonant laser pulse perpendicular to the HHG pump beam to induce uniform Rabi oscillations (periodic population oscillations between the g and e states) [34]. The Rabi oscillations serve, in this case, as a temporal periodic grating from which the pump diffracts nonlinearly to emit the HHG emission in phase [13]. Alternatively—for spatial QPM—the medium can be irradiated perpendicularly to the HHG pump beam with a chirped laser pulse inducing rapid adiabatic passage (RAP—where all the ground state population is transferred to the excited state) [14] through a mask of periodically spaced slits. In this case a spatial periodic grating of electronic state's population is established. These schemes are depicted in Fig. 2.

We choose to demonstrate this concept numerically in rubidium vapor medium as it is easily subject to coherent control. However, this technique is quite general and can be applied to other systems as well. The bound states to be controlled are the $5S_{1/2}$ and $5P_{1/2}$ states (defining the D_1 absorption line) with a transition wavelength of 795 nm.

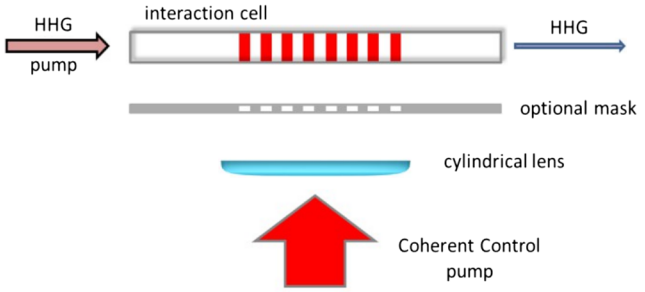

FIG. 2 (color online). Proposed setup for QPM of HHG using bound-states coherent control: A HHG pump pulse propagates along the interaction axis generating high-order harmonics. A coherent control pulse is focused uniformly using a cylindrical lens upon the interaction axis within an interaction cell, modulating the atomic population of the medium either in space by generating a quasi-static spatial population grating (with the aid of the additional mask) or in time by generating a temporal population grating through Rabi oscillations (without the mask).

The HHG pump is set to be far off-resonance with a relatively long wavelength of 2.6 μm. This reduces absorption of the HHG pump, but more importantly—the high-order harmonics are generated in the visible and ultraviolet wavelengths and there is no need for a vacuum based setup. Similar wavelength scaled versions of HHG in rubidium were demonstrated experimentally [18,35].

In the simulation the rubidium vapor pressure is 0.1 torr, corresponding to 1.9583×10^{15} atoms/cm^3, attainable for a temperature of 220 °C. Such a relatively low pressure provides very small dispersion difference between the HHG pump and harmonics (they are all far off-resonance). In order to observe phase mismatch effects over centimeter length scales, an argon buffer gas at a pressure of 600 torr is added to the simulated interaction cell. The phase mismatch is dominated by the buffer gas which is not ionized by the HHG pump beam (as its ionization potential is much higher than that of rubidium). As such, for this system, the dispersion is constant in time and $\Delta\phi_e = \Delta\phi_g$. Using a known Sellmeier equation [36] the coherence length between the HHG pump and the 13th harmonic is calculated to be 877 μm.

For temporal QPM the coherent control beam is set to induce Rabi oscillations in the medium oscillating at the generalized Rabi frequency $\Omega_R = \sqrt{\Omega^2 + \Delta^2}$, where $\Omega = \mu_{ge}E/\hbar$ is the Rabi frequency dependent upon the transition dipole moment μ_{ge} and the amplitude of the coherent control pump E. Δ is the frequency detuning from exact resonance. The generalized Rabi frequency should match the value of the temporal phase mismatch. We choose to phase match the 13th harmonic (wavelength of 200 nm) whose temporal phase mismatch is calculated, using Eq. (2), to be 1.075×10^{12} rad/s which is about 0.15% of the HHG pump frequency. To reduce the absorption of the coherent control pump, a frequency detuning of $\Delta = 0.08\Omega$ is used. Using the tabulated value of μ_{ge} [37], the required field intensity is 1.1×10^7 W/cm^2. The coherent control pulse is applied in the form of a hyperbolic secant pulse with a pulse width (FWHM) of 0.1 ns which is much longer than required for an interaction length of 1 cm yet shorter than the dephasing time of the system which is calculated (taking into account Doppler and pressure broadening) to be 0.5 ns. Propagation of the coherent control pump and the induced electronic population dynamics are calculated by numerically integrating the Maxwell-Bloch equations [34] using the fourth-order Runge-Kutta (RK4) method. The propagation is calculated along 5 mm from the side entrance of the interaction cell to the propagation axis of the HHG pump, where the Rabi oscillations are needed for QPM. The results of this simulation are shown in Fig. 3. The pulse envelope is perturbed, however, the induced Rabi oscillations around the peak of the pulse are at the required frequency, and they are maintained at this frequency within variations of less than 10% for about 50 ps, longer than the required 33 ps for allowing the HHG pump beam to interact with a uniform temporal grating along a propagation length of 1 cm.

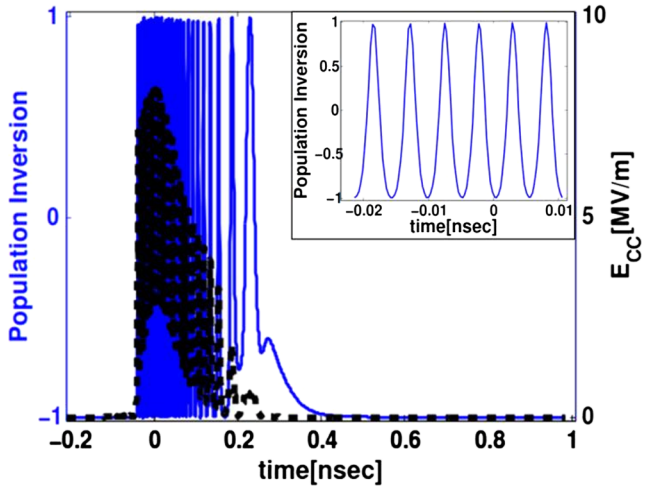

FIG. 3 (color online). Rabi oscillations induced by a coherent control electric field propagating in the medium. The black dashed line shows the coherent control field envelope after propagating 5 mm in the medium. The blue solid line shows the population inversion in the medium induced by the coherent control field. The inset shows a close up of the population inversion around the peak of the pulse, showing periodic oscillations with the desired generalized Rabi frequency.

For spatial QPM, the coherent control pump is set to induce RAP through a slitted mask. For RAP, a chirped pulse with a slow (adiabatic) frequency sweep around the relevant transition resonance of the medium can be used. The pulse parameters should satisfy the adiabaticity condition [14] $|\dot{\Omega}\Delta - \dot{\Delta}\Omega| \ll 2(\Omega^2 + \Delta^2)^{3/2}$, where the dots stand for time derivatives. For the simulation, total population inversion via RAP behind the slits of the mask is assumed, resulting in a rectangular periodic grating of electron population.

For the full simulation, the medium is prepared by the coherent control pump while the HHG pump is propagating. The 2.6 μm HHG pump duration is set to be 25 fs and its peak intensity is 2×10^{12} W/cm^2, corresponding to the cutoff at the 17th harmonic.

The propagation of the HHG pump through the medium has been simulated using the propagation equation of Geissler *et al.* [38] with an additional dispersion term for the buffer gas. The harmonics generation has been simulated through the solution of the one-dimensional Schrödinger equation using the split step method. The initial state for the solution of the Schrödinger equation at every propagation coordinate is determined through the coherent control scheme.

The results of the simulations are shown in Fig. 4. In Fig. 4(a), the HHG spectrum at the end of the interaction length is plotted for no QPM (solid black line), for temporal QPM (dashed blue line) and for spatial QPM (dash-dotted red line). The enhancement for the quasi-phase-matched

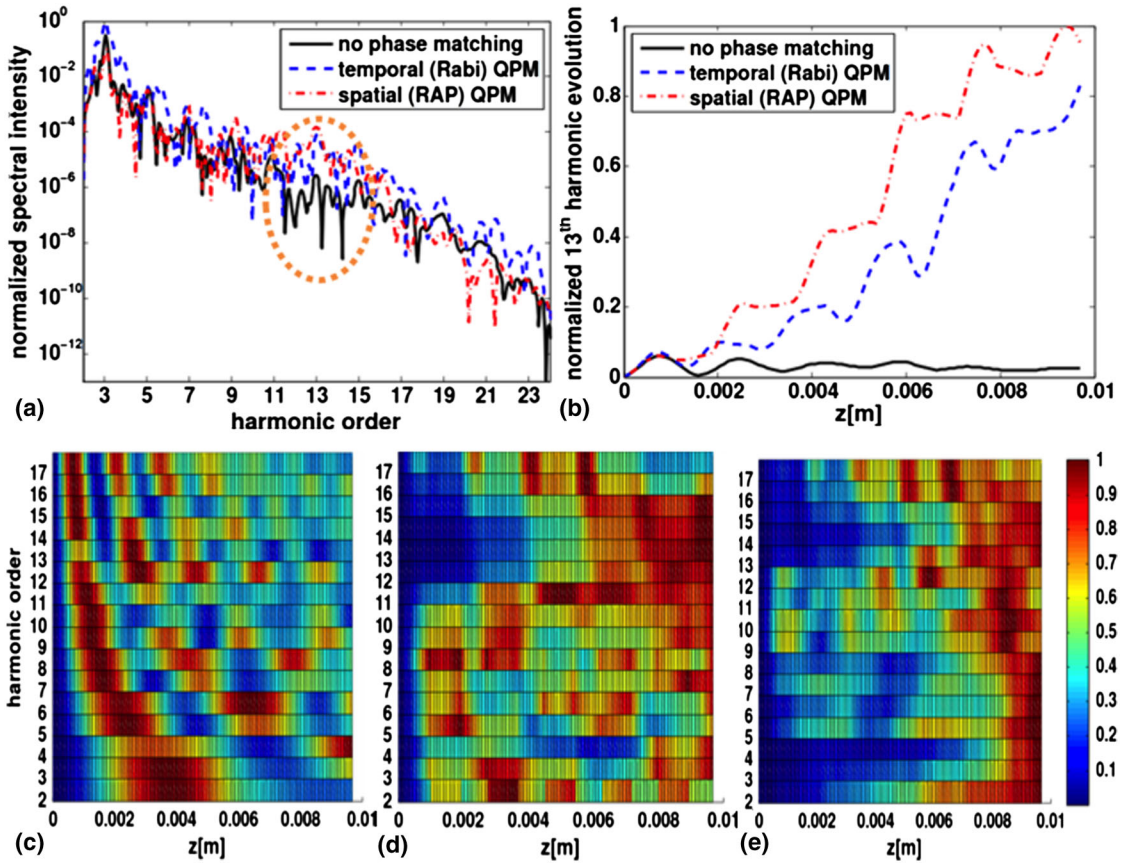

FIG. 4 (color online). QPM of HHG using bound states' coherent control. (a) Harmonic spectrum at the end of the interaction cell, normalized to the strongest harmonic emission. (b) Thirteenth harmonic evolution along the HHG pump propagation direction, normalized to the strongest enhancement during the propagation. The solid black line represents propagation in a medium with no QPM, the dashed blue line represents propagation in a medium with temporal QPM prepared with Rabi oscillations and the dash-dotted red line represents propagation in a medium with spatial QPM prepared with RAP and a mask of slits. (c),(d),(e): Evolution of the HHG spectrum, normalized for each harmonic order separately, with (c) no QPM, (d) spatial QPM, and (e) temporal QPM.

13th harmonic is about 2 orders of magnitude compared with the non-phase-matched case. In Fig. 4(b) the evolution of the 13th harmonic as a function of propagation is plotted for the same three cases. For the QPM cases, a characteristic growth is observed, while for the non-QPM case the regular oscillatory evolution is observed. Figures 4(c), 4(d) and 4(e) show the buildup intensity of all the harmonic orders below the cutoff for no QPM, spatial QPM, and temporal QPM, respectively. When no QPM is applied an oscillating pattern for all harmonic orders is observed—each with its associated periodicity of $2\pi/\Delta k$. With spatial QPM the harmonic orders around the 13th harmonic are being built while the other harmonics still oscillate along the interaction coordinate. For the case of temporal QPM, due to the use of a sinusoidal modulation of the population, a strong response at the transition frequency of the D1 line is observed as well.

In summery, we have shown that manipulating the bound state population of a medium's atoms can be used for macroscopic control over the process of HHG. This can be done by either employing a spatial or a temporal grating of atomic bound state population in the medium. The temporal grating is interesting due to two reasons: First, it supplies a framework for the realization of temporal QPM, which is yet to be demonstrated experimentally. Second, it is a highly tunable method for phase matching. To phase match different harmonic orders, one simply has to modify the amplitude or detuning of the coherent control beam. Two different regimes of coherent control were used together in this work—coherent control between bound states and attosecond coherent control manifested in the process of HHG where the control is applied to both a bound state and the continuum. Such a combination might be useful for quantum tomography [39,40] using the ability of the presented macroscopic control scheme to isolate specific HHG channels in an ionization dominant excited medium. Alternatively it would be interesting to use a temporal population grating to map the radiation emitted from an excited medium onto frequency shifted orders (as the temporal analogue to diffraction from spatial gratings onto crystal-momentum shifted orders). Further directions worth exploring are extension of the presented concepts to cases

of multiple excited states and to the application of more elaborate coherent control schemes, involving spatiotemporal population modulation and accelerating modulations [41]. In addition, extension of the underlying ideas to other media and settings is also possible. Examples are molecular systems, noble gases with the application of multiphoton Rabi oscillations, initially excited noble gases or application of an EUV source for coherent control.

This work was supported by the Israeli Science Foundation, Grant No. 1233/13.

*alonb@eng.tau.ac.il

[1] H. Kapteyn, O. Cohen, I. Christov, and M. Murnane, Science **317**, 775 (2007).
[2] P. B. Corkum and F. Krausz, Nat. Phys. **3**, 381 (2007).
[3] F. Krausz and M. Ivanov, Rev. Mod. Phys. **81**, 163 (2009).
[4] J. A. Armstrong, N. Bloembergen, J. Ducuing, and P. S. Pershan, Phys. Rev. **127**, 1918 (1962).
[5] A Paul, R. A. Bartels, R. Tobey, H. Green, S. Weiman, I. P. Christov, M. M. Murnane, H. C. Kapteyn, and S. Backus, Nature (London) **421**, 51 (2003).
[6] E. A. Gibson *et al.*, Science **302**, 95 (2003).
[7] J. Seres, V. S. Yakovlev, E. Seres, Ch. Streli, P. Wobrauschek, Ch. Spielmann, and F. Krausz, Nat. Phys. **3**, 878 (2007).
[8] A. Willner *et al.*, Phys. Rev. Lett. **107**, 175002 (2011).
[9] M. Zepf, B. Dromey, M. Landreman, P. Foster, and S. M. Hooker, Phys. Rev. Lett. **99**, 143901 (2007).
[10] X. Zhang, A. L. Lytle, T. Popmintchev, X. Zhou, H. C. Kapteyn, M. M. Murnane, and O. Cohen, Nat. Phys. **3**, 270 (2007).
[11] A. L. Lytle, X. Zhang, R. L. Sandberg, O. Cohen, H. C. Kapteyn, and M. M. Murnane, Opt. Express **16**, 6544 (2008).
[12] R. Lifshitz, A. Arie, and A. Bahabad, Phys. Rev. Lett. **95**, 133901 (2005).
[13] A. Bahabad, M. M. Murnane, and H. C. Kapteyn, Nat. Photonics **4**, 570 (2010).
[14] N. V. Vitanov, T. Halfmann, B. W. Shore, and K. Bergmann, Annu. Rev. Phys. Chem. **52**, 763 (2001).
[15] B. W. Shore, Acta. Physica Slovaca, Reviews and Tutorials **58**, 243 (2008).
[16] A. K. Gupta and D. Neuhauser, Chem. Phys. Lett. **290**, 543 (1998).
[17] B. Wang, T. Cheng, X. Li, P. Fu, S. Chen, and J. Liu, Phys. Rev. A, **72**, 063412 (2005).
[18] P. M. Paul, T. O. Clatterbuck, C. Lyngå, P. Colosimo, L. F. DiMauro, P. Agostini, and K. C. Kulander, Phys. Rev. Lett., **94**, 113906 (2005).
[19] I. A. Ivanov and A. S. Kheifets, J. Phys. B **41**, 115603 (2008).
[20] Ji-Gen Chen, Yu-Jun Yang, Si-Liang Zeng, and Hua-Qiu Liang, Phys. Rev. A **83**, 023401 (2011).
[21] Y. Yu-Jun, CHEN Ji-Gen, CHI Fang-Ping, ZHU Qi-Ren, ZHANG Hong-Xing, and Sun Jia-Zhong, Chin. Phys. Lett. **24**, 1537 (2007).
[22] V. A. Antonov, Y. V. Radeonychev, and O. Kocharovskaya, Phys. Rev. Lett. **110**, 213903 (2013).
[23] A. Sanpera, J. B. Watson, M. Lewenstein, and K. Burnett, Phys. Rev. A **54**, 4320 (1996).
[24] J. B. Watson, A. Sanpera, X. Chen, and K. Burnett, Phys. Rev. A **53**, R1962 (1996).
[25] S. Chelkowski, T. Bredtmann, and A. D. Bandrauk, Phys. Rev. A **85**, 033404 (2012).
[26] S. Chelkowski, T. Bredtmann, and A. D. Bandrauk, Phys. Rev. A **88**, 033423 (2013).
[27] C. Figueira de Morisson Faria, M. Dörr, and W. Sandner, Phys. Rev. A **58**, 2990 (1998).
[28] J. Bao, W. Chen, Z. Zhao, and J. Yuan, J. Phys. B **44**, 195601 (2011).
[29] Y. Mairesse, D. Zeidler, N. Dudovich, M. Spanner, J. Levesque, D. M. Villeneuve, and P. B. Corkum, Phys. Rev. Lett. **100**, 143903 (2008).
[30] A Rupenyan, J. B. Bertrand, D. M. Villeneuve, and H. J. Wörner, Phys. Rev. Lett. **108**, 033903 (2012).
[31] H. J. Worner, J. B. Bertrand, D. V. Kartashov, P. B. Corkum, and D. M. Villeneuve, Nature (London) **466**, 604 (2010).
[32] H. J. Wörner *et al.*, Science **334**, 208 (2011).
[33] K. Hartinger, S. Nirmalgandhi, J. Wilson, and R. Batels, Opt. Express **13**, 6919 (2005).
[34] Peter W. Milonni and J. H. Eberly, *Laser Physics* (Wiley, New York, 2010).
[35] B. Sheehy, J. D. D. Martin, L. F. DiMauro, P. Agostini, K. J. Schafer, M. B. Gaarde, and K. C. Kulander, Phys. Rev. Lett. **83**, 5270 (1999).
[36] A. Börzsönyi, Zs. Heiner, M. P. Kalashnikov, A. P. Kovács, and K. Osvay, Appl. Opt. **47**, 4856 (2008).
[37] D. A. Steck, Rubidium 85 d line data, http://steck.us/alkalidata/rubidium85numbers.pdf, 2008.
[38] M. Geissler, G. Tempea, A. Scrinzi, M. Schnürer, F. Krausz, and T. Brabec, Phys. Rev. Lett. **83**, 2930 (1999).
[39] S. Haessler *et al.*, Nat. Phys. **6**, 200 (2010).
[40] J. Itatani, J. Levesque, D. Zeidler, H. Niikura, H. Pépin, Jean-Claude Kieffer, P. B. Corkum, and D. M. Villeneuve, Nature (London) **432**, 867 (2004).
[41] A. Bahabad, M. M. Murnane, and H. C. Kapteyn, Phys. Rev. A **84**, 033819 (2011).